



Mössbauer study and structural characterization of $\text{UO}_2\text{-Gd}_2\text{O}_3$ sintered compounds

L. Pagano Jr.^a, G.P. Valença^a, S.L. Silva^b, A.E.L. Cláudio^b, F.F. Ivashita^c, R. Barco^c,
S.N. de Medeiros^c, A. Paesano Jr.^{c,*}

^a Faculdade de Engenharia Química, Universidade Estadual de Campinas, Brazil

^b Laboratório de Materiais Nucleares, Centro Tecnológico da Marinha, ARAMAR, SP, Brazil

^c Departamento de Física, Universidade Estadual de Maringá, PR, Brazil

ARTICLE INFO

Article history:

Received 24 September 2007

Accepted 31 March 2008

PACS:

28.41

64.75

66.30

ABSTRACT

Samples of UO_2 and up to 10 wt% of Gd_2O_3 were prepared by solid-state reaction under a reducing atmosphere, in a thermal path comprising ramps and dwell times in the temperature range of 900–1750 °C. The sintered material was analyzed by X-ray diffraction and ^{155}Gd Mössbauer spectroscopy. The results showed that for samples annealed up to 900 °C, the gadolinium sesquioxide remained unreacted. However, when the temperature was increased to 1300 °C, a solid-state reaction took place forming mixed oxides. For the more severe sintering condition, at 1750 °C, gadolinia left urania partially unreacted producing a material consisting of two compositions, UO_2 (with no dissolved gadolinium) and $(\text{U,Gd})\text{O}_2$. The proposed heating cycle provided pellets free from Gd_2O_3 phase and may be used by the nuclear fuel industry as a suitable sintering process.

© 2008 Elsevier B.V. All rights reserved.

1. Introduction

The nuclear fuel $\text{UO}_2\text{-Gd}_2\text{O}_3$ has been widely used because of the improvement in the reactor performance and the extension of burn-up in light water reactors (LWR). Gadolinium is a burnable absorber that provides a negative moderator coefficient, i.e., it has a high macroscopic neutron absorption cross-section and is able to suppress the initial excess of reactivity at the beginning of the core life in LWR [1–4].

Usually, the $\text{UO}_2\text{-Gd}_2\text{O}_3$ pellets are prepared by sintering a mixture of mechanically blended powders of UO_2 and up to 10 wt% of Gd_2O_3 , and the obtained materials are expected to be mostly solid solutions of the $(\text{U,Gd})\text{O}_2$ type [5–8]. Optimal microstructure characteristics of the solid solutions can be obtained by several process routes, dry or wet, which may result in materials with significantly different characteristics and properties [5,8,9]. In general, $\text{UO}_2\text{-Gd}_2\text{O}_3$ pellets present smaller grain size, thermal diffusivity and density, in comparison with UO_2 fuel pellets prepared in the same sintering conditions [6,10,11].

In spite of the high sintering temperature (~ 1700 °C), inhomogeneous gadolinium distribution can occur and Gd_2O_3 clusters may be found at the sintered pellet. This is very undesirable, because Gd_2O_3 clusters will cause internal cracks and porosity in the pellets, which, in turn, will affect fuel performance and, eventually,

cause fuel rod failure. Moreover, the self shielding effect will prevent the gadolinium atoms inside the clusters from taking part in the nuclear reaction, and only those at the boundaries will stand a chance of absorbing neutrons. As a result, the effective amount of burnable poison at the early stages of core life, when the reactivity is the highest, will be less than that expected from the mean composition. This effect must be avoided for the sake of reactor safety.

In order to reduce the presence of these clusters and their deleterious effects, the interdiffusion of gadolinia in the urania matrix has to be almost complete at the end of the sintering process. Indeed, the fabrication of a nuclear fuel has to accomplish several requirements, as established by the nuclear reactor design, and one of them is the maximum size of the remaining gadolinia segregates [7]. The understanding of the interdiffusion kinetics is of utmost importance in designing the fuel sintering process, i.e., in establishing a temperature profile and a set of sintering additives, suitable to achieve the required fuel characteristics.

Several techniques have been used to probe the interdiffusion kinetics of gadolinium in the UO_2 matrix and the presence of non-exhausted gadolinia. In particular, X-ray diffraction (XRD) and scanning electron microscopy (SEM) have been the most frequent characterization techniques employed to analyze the chemical homogeneity in $\text{UO}_2\text{-Gd}_2\text{O}_3$ pellets [12,13].

However, homogeneity is a question of scale and it is possible that very fine particles can remain undissolved after sintering the pellets. In this case, i.e., with inhomogeneity in nanoscale, neither XRD nor SEM are capable to reliably distinguish this kind of nanometric particles since the former requires long range order and the latter has resolution limited to micrometric scale.

* Corresponding author. Tel./fax: +55 44 32634623.

E-mail address: paesano@wnet.com.br (A. Paesano Jr.).

In this sense, ‘microscopic’ techniques potentially capable to see at nanoscopic level, e.g., transmission electron microscopy (TEM) or Mössbauer spectroscopy (MS), could be applied for the above mentioned purpose. Both analytical methods are suitable for kinetics investigation because they provide quantitative data on phase distribution with outstanding resolution.

^{155}Gd is a Mössbauer isotope and, therefore, can be used as a nuclear probe for gadolinium-containing compounds such as the Gd–U–O mixed oxides that might be formed by solid-state reaction during the pellets’ heat treatment.

Thus, the main objective of the present study was to follow, by ^{155}Gd Mössbauer spectroscopy, the dissolution of Gd_2O_3 in the UO_2 matrix at the different stages of a conventional thermal cycle of fuel pellet sintering.

The fuel pellets analysed in this study were previously characterized by optical microscopy, SEM, thermal analysis (TG, DTA, DSC, dilatometry and thermal diffusivity) and ordinary XRD and the results have been reported [14,15]. The experiments performed at the Nuclear Materials Laboratory (CTMSP-BRAZIL) revealed, in brief, that the fabricated fuel presents high microstructural homogeneity with additions of Gd_2O_3 up to 10 wt%, demonstrating the suitability of the ceramic processing adopted in the production of this material.

The hyperfine characterization of UO_2 – Gd_2O_3 fuel through MS, together with meticulous XRD measurements on sintered UO_2 – Gd_2O_3 pellets, according to our knowledge, is first reported in this paper.

2. Experimental details

Three batches of blended samples were prepared: $\text{UO}_2 \cdot X\text{wt}\% \text{Gd}_2\text{O}_3$, with $X = 3, 7$ and 10 . For comparison, one batch of pellets of ‘pure’ UO_2 was prepared. The $\text{UO}_2 + \text{Gd}_2\text{O}_3$ powders were blended by mixing the precursors in a turbula mixer at 32 rpm, for 4 h. The UO_2 used to prepare all samples was an ex-ammonium uranyl carbonate powder with impurity content less than 150 ppm, specific surface area (BET) of $5.7 \pm 0.1 \text{ m}^2/\text{g}$, average particle size of $7.4 \pm 0.2 \mu\text{m}$ (Sedigraph), and O/U ratio of 2.15 ± 0.01 . The Gd_2O_3 raw powder was of commercial grade (i.e., 99.95% pure), with average particle size of $2.7 \pm 0.2 \mu\text{m}$ and was calcinated under $900^\circ\text{C}/2 \text{ h}$ before mixing.

The pellets were pressed in composition batches, where ‘green’ pellets were obtained in pressures varying from 350 up to 400 MPa. The pressing process was done in a floating table press, having green densities in the range 51–53% theoretical density.

The sintering cycle was conducted under a 99.999% H_2 atmosphere, at a flow of 200 ml/min, in a vertical molybdenum furnace, raising the temperature up to 1750°C . All composition batches were run in a single thermal cycle operation, comprising ramps and dwell times, as shown in Fig. 1. However, sampling pellets were removed from the furnace at some intermediary points (i.e., without completing the cycle). Then, the pellets were ground for the sake of characterization.

The X-ray diffractograms were measured using $\text{Cu K}\alpha$ radiation, on a Phillips X-Pert Diffractometer (PW3710), in the conventional θ – 2θ geometry. The diffraction data were analyzed by the Rietveld method (FullProf Code). A few measurements were taken using the synchrotron light at LNLS (Campinas – Brazil), using a wavelength of 0.154115 nm .

The MS in gadolinium was performed using the 86.5 keV transition of the ^{155}Gd nucleus, with the spectra acquired at 5 K, in a helium flow cryostat. The $^{154}\text{Sm}(^{155}\text{Eu})\text{Pd}_3$ source was irradiated in the research reactor at IPEN – São Paulo, Brazil, and assembled at the CTMSP Nuclear Materials Laboratory. The source was moved vertically with a sinusoidal velocity toward the absorbers, which

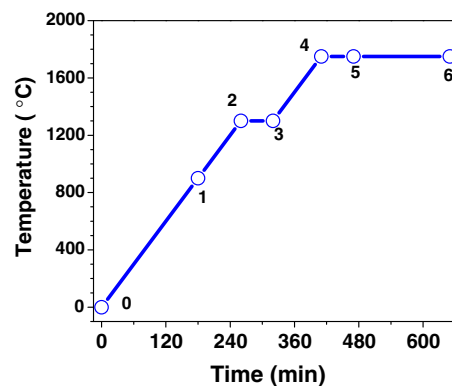


Fig. 1. Thermal cycle of the $\text{UO}_2 + \text{Gd}_2\text{O}_3$ sintered samples: (1) annealing up to 900°C ; annealing up to 1300°C , without (2) and with (3) a temperature dwell time of 1 h; annealing up to 1750°C , without (4) and with temperature dwell times of 1 h (5) and 4 h (6); Point 0 is for green pellets (i.e., without sintering).

usually had 300 mg cm^{-2} . The Mössbauer γ -rays were detected with a Ge (HP) solid-state detector and the velocity scale was calibrated with a $^{57}\text{Co}(\text{Rh})$ and a metallic iron foil at room temperature. The Mössbauer transmission spectra were analyzed with a non-linear least-square routine, with a Lorentzian line shape modified by a ζ dispersive term for ^{155}Gd [16].

3. Results and discussion

3.1. X-ray diffraction

The X-ray pattern for the UO_2 –7 wt% Gd_2O_3 sample sintered up to $1750^\circ\text{C}/4 \text{ h}$ (Point 6 in Fig. 1) is shown in Fig. 2. The diffractogram was refined considering two isomorphous structures, one of them being the UO_2 phase.

Fig. 3 shows the peak analysis for two particular angular regions, the (220) and (331) reflection planes of the urania pattern, as obtained from a scan for the same earlier sample (Fig. 3(b)) and, also, for the UO_2 sintered sample (Fig. 3(a)).

The continuous curves under the experimental (dotted) profiles are the result of the fit considering the $K_{\alpha 1}$ and $K_{\alpha 2}$ radiations individually. The peaks for both components were taken as having pure Lorentzian shapes, with areas constrained in the ratio 2:1, centroids related by $K_{\alpha 1} \cdot \sin\theta_{\alpha 1} = \sin\theta_{\alpha 2} \cdot K_{\alpha 2}$ and with a common linewidth [17].

It can be seen that whereas for the fit of the pure UO_2 sample only one pair was necessary, the scan of the mixed sample required two pairs of $K_{\alpha 1}$ and $K_{\alpha 2}$ components. Although the angular region is coincident, the pair of lines on the right side in Fig. 3(b) cannot be attributed to gadolinia peaks since a careful inspection reveals the absence of other gadolinia peaks in their expected angular positions. This situation is observed for all other experimental peaks in the diffractogram of Fig. 2 as well as in the diffractograms of the samples with 3% and 10% of gadolinia, equally heat-treated (i.e., obtained at Point 6). Thus, the pair of peaks existing beside every urania pair of peaks may be attributed to a solid solution of the $(\text{U,Gd})\text{O}_2$ type, which co-exists with the ‘pure’ UO_2 phase.

The evolution of the peaks for the (111) and (311) reflection planes can be followed in Fig. 4, where scans at the respective angular regions, obtained by diffraction of synchrotron light, are presented.

It can be seen that the peaks shift to the left for the initial steps of the sintering route and then return to the right. At the end of the thermal cycle, a pair of peaks (red line) is visible for each reflection plane. The single wavelength of the synchrotron source makes the occurrence of two isomorphous structures irrefutable.

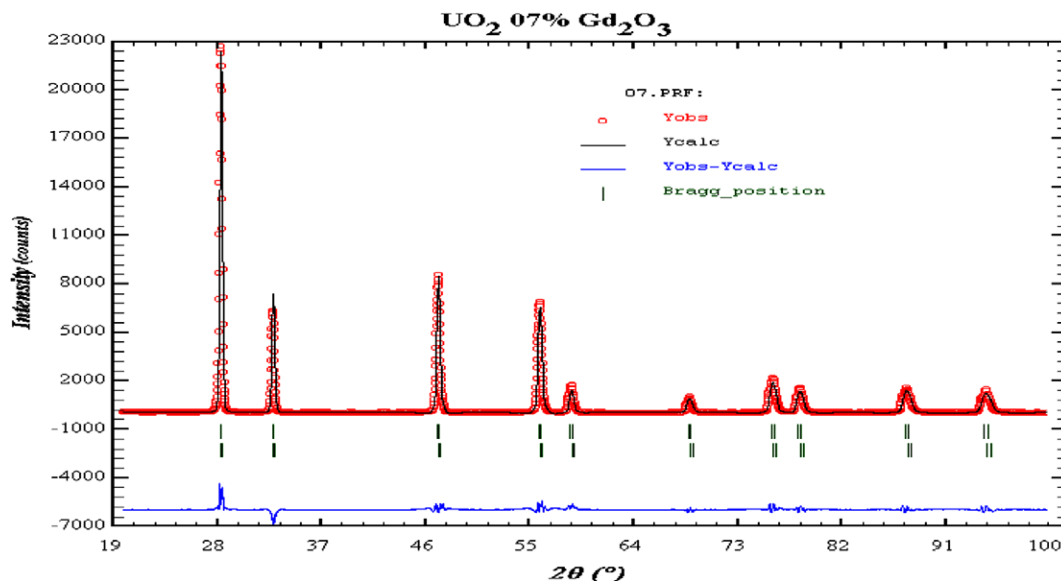


Fig. 2. Refined X-ray pattern for the UO_2 -7 wt% Gd_2O_3 sample sintered up to 1750 °C/4 h.

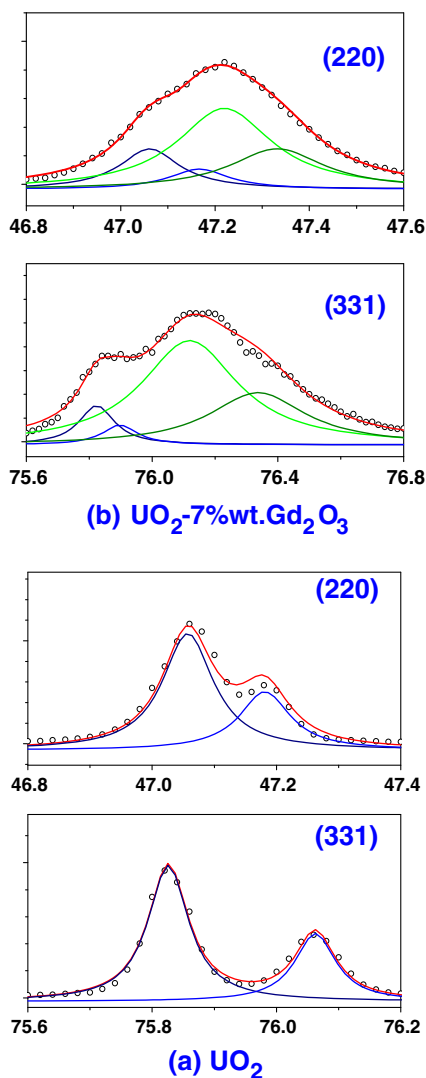


Fig. 3. Scans of the (220) and (331) reflection planes for the UO_2 and UO_2 -7 wt% Gd_2O_3 samples sintered at 1750 °C/4 h.

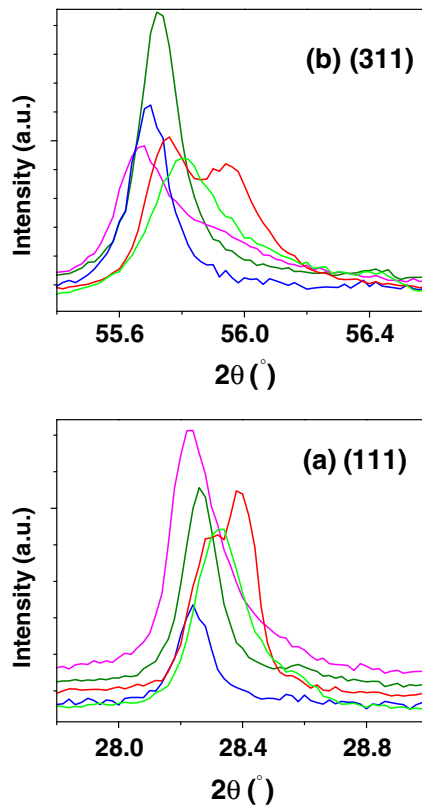


Fig. 4. Scans of the (111) (a) and (311) (b) reflection planes for the UO_2 -7 wt% Gd_2O_3 sintered samples, as measured using synchrotron light, at different stages of the thermal cycle of sintering: **green** Point 0; **dark green** Point 2; **blue** Point 3; **magenta** Point 4; **red** Point 6.

3.2. Mössbauer analysis

The Mössbauer spectra for the gadolinia precursor, as measured in this study, and for some selected UO_2 - Gd_2O_3 sintered samples, are shown in Figs. 5 and 6, respectively. The fitted hyperfine parameters for the sintered samples, as well as for the precursor, are presented in Table 1. The values obtained for Gd_2O_3 (i.e., the

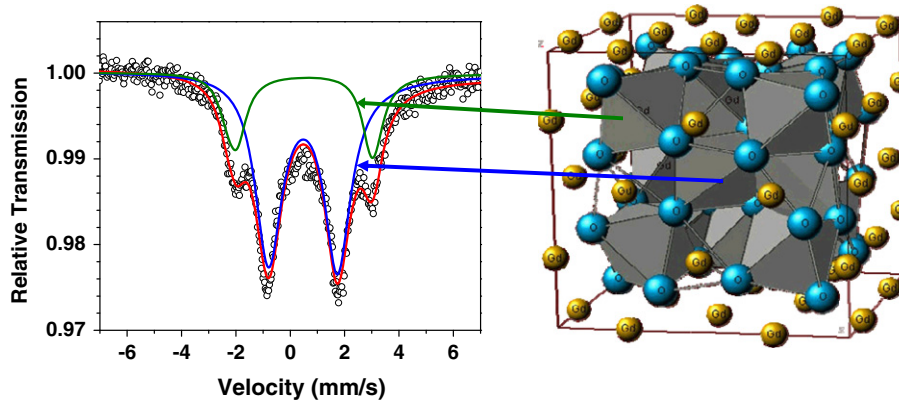


Fig. 5. Mössbauer pattern and the unit cell of gadolinia. The gadolinium cations occupy two octahedral sites, 24d (blue line) and 8b (green line). The arrows connect each subspectral component with the polyhedral coordination of the respective site. (For interpretation of the references to colour in this figure legend, the reader is referred to the web version of this article.)

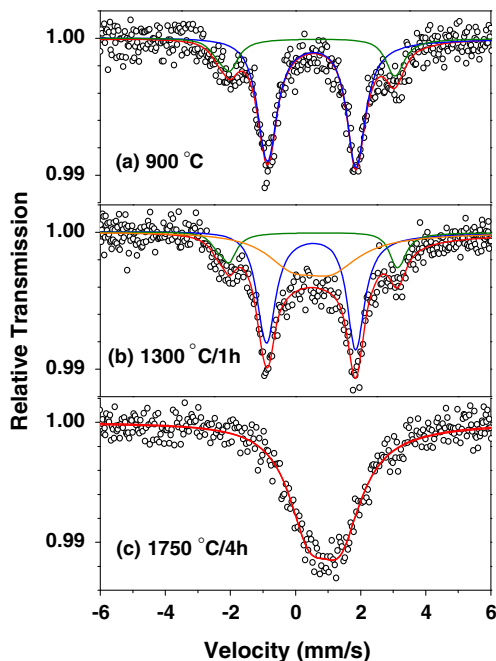


Fig. 6. ^{155}Gd Mössbauer spectra taken at 5 K for the UO_2 -7 wt% Gd_2O_3 sintered samples.

quadrupole splitting – QS – and the isomer shift – IS) are in good agreement with those reported earlier [16,18].

Different assumptions were taken into account in the fitting procedures, depending on the measured sample. For the sample

Table 1

Hyperfine parameters and subspectral areas for some of the UO_2 -7 wt% Gd_2O_3 sintered samples

Sample	IS (mm/s) (± 0.02)	QS (mm/s) (± 0.02)	Γ (mm/s)	η	Area (%)	
Gd_2O_3	0.45	2.60	1.16	0.90*	75.0*	
	0.47	5.39	0.85	0*	25.0*	
$\text{UO}_2 + 7 \text{ wt}\% \text{ Gd}_2\text{O}_3$	900 °C	0.48	2.80	0.66	0.90*	77.5
		0.46	5.47	0.63	0*	22.5
	1300 °C/1 h	0.46	2.83	0.62	0.90*	48.0
		0.48	5.47	0.63	0*	13.3
		0.48	1.28	1.99	0*	38.7
	1750 °C/4 h	0.87	1.01	1.56	0*	100

* Parameter constrained in the fit.

sintered up to 900 °C (Point 1 in Fig. 1), the spectrum (Fig. 6(a)) virtually reproduced the gadolinia pattern. Accordingly, two sites for gadolinium were considered, one with $\eta = 0$ and the other with $\eta = 0.9$, which are the asymmetry parameters for the gadolinium sites in gadolinia¹.

The fitted hyperfine parameters, including the relative areas (made free in the fit), practically reproduce those obtained for the gadolinia precursor. This revealed that the gadolinia in the urania matrix did not react at the pointed out heat treatment. For the sample treated up to 1300 °C/1 h (Point 3 in Fig. 1), the best fit was attained by considering three sites (Fig. 6(b)). Two of them belong to gadolinia (see Table 1), revealing that this precursor was not yet exhausted.

On the other hand, the central part of the spectrum shows the formation of some mixed U–Gd oxide, and was imposed in the fit as a single (third) site. This reacted and, certainly, complex ‘phase’ demonstrates that an interdiffusion process effectively took place due to the applied heat treatment. Far from a crystallographic ordered single compound, this component reflects the formation of layers or clusters where the gadolinium is interdiffused into the urania matrix, very probably with varying concentration. As a consequence, the gadolinium cations have a multiplicity of neighborhoods and every fitted or constrained hyperfine parameter could, at best, be considered as an ‘effective’ or average value. The spectrum of Fig. 6(b) was fitted with these assumptions.

Finally, for the most severely heat-treated sample (Fig. 6(c)), the spectrum shows a singlet pattern. In this case, it can be assumed that the gadolinium probe occupied a site with symmetry properties similar to the cubic uranium site in the urania lattice. Thus, the spectrum was fitted taking only one site into account, with the quadrupole splitting as a free parameter but η constrained to zero. The fitted values (Table 1) and fit quality showed that the above assumption is consistent with the data. Certainly, this phase corresponds to the (U,Gd) O_2 solid solution detected by XRD.

Fig. 7 shows the lattice parameters, as a function of the initial sesquioxide concentration, for UO_2 and the (U,Gd) O_2 solid solutions, as obtained from the Rietveld analysis. It can be seen that the lattice parameter of the (U,Gd) O_2 solid solution decreased linearly, which is usually attributed to oxygen vacancies, as the gadolinium enters in the urania matrix substitutional to uranium [19]. Differently, the UO_2 phase remained relatively stabilized, as the sesquioxide initial content increased. Although the lattice param-

¹ Site 8b has axial symmetry and 24d has not. The $\eta = 0.9$ was calculated considering the point charge approximation and atomic positions as provided from the Rietveld analysis of the gadolinia diffractogram.

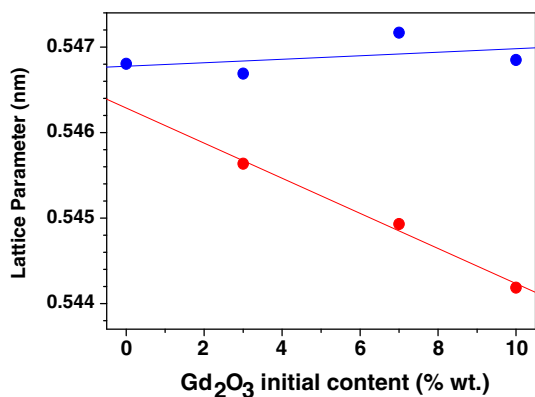


Fig. 7. Lattice parameters for the UO₂ (blue circles) and (U,Gd)O₂ (red circles) isomorphous phases, as a function of the Gd₂O₃ initial content, for the samples sintered up to 1750 °C/4 h. The straight lines are linear regression fits for the refined (lattice) parameters. (For interpretation of the references to colour in this figure legend, the reader is referred to the web version of this article.)

ter decrease was an expected result, the occurrence of, simultaneously, zero and non-zero concentrations for gadolinium throughout the sintered material has been a little reported result.

4. Conclusions

Mössbauer spectroscopy is a powerful tool to analyse the UO₂–Gd₂O₃ sintered system and to quantify the amount of free Gd₂O₃ phase left at the end of the sintering fuel cycle, if any. Combined with the Rietveld analysis of X-ray diffraction data, it was possible to detect that gadolinia remains unreacted in the UO₂–Gd₂O₃ pellets sintered up to 900 °C but it was completely dissolved at 1750 °C/4 h.

The urania–gadolinia system proceeds through an interdiffusion reaction when sintered up to 1300 °C/1 h and forms a (U,Gd)O₂ solid solution, but leaves unreacted UO₂ even after sintering by 1750 °C/4 h. The final sintered material consists of two

compositions, i.e., UO₂ (with no dissolved gadolinium) and (U,Gd)O₂.

The proposed heating cycle provided urania–gadolinia pellets free from Gd₂O₃ phase. Therefore, it might be a suitable sintering process to be used in the nuclear fuel industry.

Acknowledgements

The authors would like to thank to the Brazilian agencies, CNPq, Fundação Araucária, CAPES and to the National Laboratory of Synchrotron Light (LNLS), for financial support.

References

- [1] H. Assmann, J.P. Robin, in: Guidebook on Quality Control of Mixed Oxides and Gadolinium Bearing Fuels for Light Water Reactors, IAEA-TECDOC-584, IAEA, Vienna, 1983. p. 51.
- [2] H. Markl, R. Holzer, *Kerntechnik* 50 (1987) 241.
- [3] T. Wada, K. Noro, K. Tsukui, in: Proceedings of the International Conference on Nuclear Fuel Performance, London, UK, 1973.
- [4] R. Manzel, W.O. Dörr, *Am. Ceram. Soc. Bull.* 59 (1980) 601.
- [5] H.G. Riella, M. Durazzo, M. Hirata, R.A. Nogueira, *J. Nucl. Mater.* 178 (1991) 204.
- [6] R. Yuda, K. Une, *J. Nucl. Mater.* 178 (1991) 195.
- [7] C. Miyake, M. Kanamaru, S. Imoto, *J. Nucl. Mater.* 138 (1986) 142.
- [8] TECDOC-844, International Atomic Energy Agency, Characteristics and Use of Urania-Gadolinia Fuels, ISSN 1011-4289, Vienna, Austria, 1995.
- [9] G. Gündüz, I. Uslu, I.I. Önal, H.H. Durmazucar, T. Öztürk, A.A. Aksit, B. Kopuz, F. Can, S. Can, R. Uzmen, *Nucl. Technol.* 11 (1995) 63.
- [10] Kun Woo Song, Keon Sik Kim, Ki Won Kang, Youn Ho Jung, *J. Nucl. Mater.* 317 (2003) 204.
- [11] M. Hirai, *J. Nucl. Mater.* 173 (1990) 247.
- [12] L. Hälldahl, S. Eriksson, *J. Nucl. Mater.* 153 (1988) 66.
- [13] A.G. Leyva, D. Vega, V. Trimarco, D.J. Marchi, *J. Nucl. Mater.* 303 (2002) 29.
- [14] T.A. Restivo, A.E. Cláudio, E.E. Silva, L. Pagano Jr., in: TECDOC-1416, International Atomic Energy Agency, 'Advanced Fuel Pellet Materials and Designs for Water Cooled Reactors', ISSN 1011-4289, Vienna, Austria, 2004, p. 147.
- [15] T.A. Restivo, L. Pagano Jr., in: Proceedings of the Conference on Characterization and Quality Control of Nuclear Fuels, ISBN 81-7764-608-7, Allied Publishers, New Delhi, India, 2004, p. 139.
- [16] G. Czjzek, in: G.J. Long, F. Grandjean (Eds.), Mössbauer Spectroscopy Applied to Magnetism and Materials Science, Plenum, New York, 1993 (Chapter 9).
- [17] B.D. Cullity, *Elements of X-ray Diffraction*, Addison-Wesley, 1967.
- [18] J.D. Cashion, D.B. Prowse, A. Vas, *J. Phys. C: Solid State Phys.* 6 (1973) 2611.
- [19] T. Ohmichi, S. Fukushima, A. Maeda, H. Watanabe, *J. Nucl. Mater.* 102 (1981) 40.